COASTING BEAM TRANSVERSE COHERENT INSTABILITIES

J.L. Laclare
ESRF, Grenoble, France

Abstract
Nowadays, the performance of most machines is limited by Coherent Instabilities. It is one of the most important collective effects which prevents the current from being increased above a certain threshold without the beam quality being spoiled. For the transverse instabilities we will follow a very similar approach to the longitudinal case in the previous chapter. Thus, a large number of basic explanations and comments again apply and will not be repeated. Wherever relevant we will insist on the differences. With regard to the scope of the lecture, the physical mechanisms which will be considered throughout can be applied to any type of machine :
- linear accelerators,
- circular accelerators,
- storage rings

and beam:
- bunched beams
- continuous beams.

1. INTRODUCTION

In the longitudinal plane, the coherent motion is driven by a longitudinal modulation of particle density which creates a longitudinal electric field along the beam axis. When reverting back to the example of the round pipe, this self field is associated with a return or image current I_W flowing downstream and uniformly distributed on the inner side of the chamber wall.

In the transverse case, we will arbitrarily choose the X plane, the perturbation consists of a slight initial transverse displacement of the beam. Due to the focusing of the external guide field, the beam then oscillates from side to side when progressing along the machine.

The first remark is that the total wall current I_W has the same magnitude as before but is no longer uniformly distributed in the wall. When comparing the new situation with the unperturbed one, the beam sees a differential current $\pm \delta I_W$ which flows in the opposite direction on either side of the pipe.

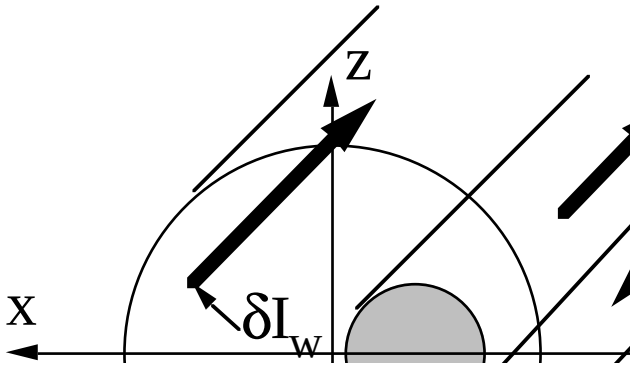

Fig. 1

This requires a longitudinal electric field, which varies linearly in strength across the

aperture, and also a vertical and constant dipole magnetic field. This magnetic field acts back on the beam.

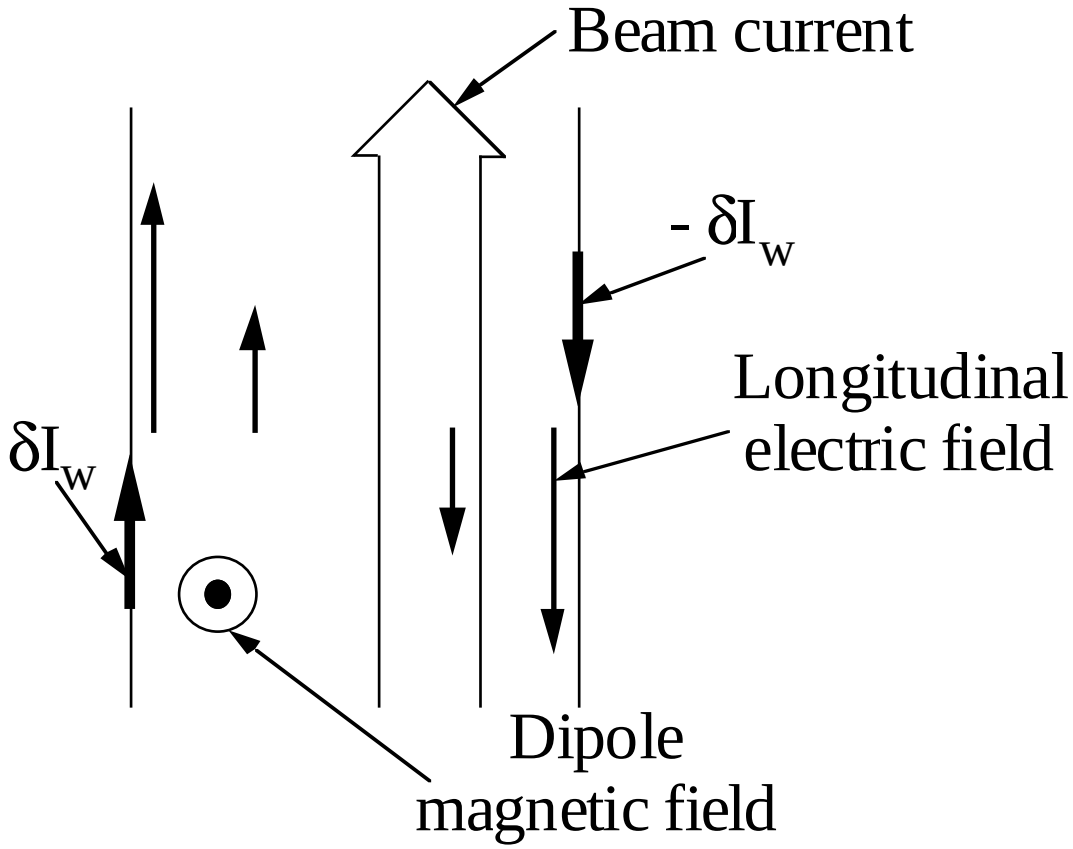

Fig. 2

This magnetic field can either:

– increase the initial displacement thus leading to an instability, or,
– reduce the initial displacement and therefore stabilize the beam.

2. SINGLE-PARTICLE TRANSVERSE MOTION

The transverse unperturbed motion is described in the following form:

$$\ddot{x} + \dot{\varphi}^2 x = 0 \tag{1}$$

where $\dot{\varphi} = \omega_\beta = Q_x \omega$ is the betatron advance per second, Qx the particle horizontal tune, and ω the particle revolution frequency.

The transverse position will be expressed as:

$$x(t) = \hat{x}\cos\varphi(t) = \hat{x}\cos\left[\int_0^t \dot{\varphi}\, dt + \varphi_0\right] \tag{2}$$

The couple $\{\varphi , \hat{x}\}$ instead of $\{x , \dot{x}\}$ will be used for the description of the transverse

motion in canonical variables.

$$\dot{\varphi} = \frac{d\varphi}{dt} \text{ and } \hat{x} = \left[x^2 + \left(\frac{\dot{x}}{\dot{\varphi}}\right)^2 \right]^{\frac{1}{2}} \tag{3}$$

are two invariants of the unperturbed motion.

Both parameters Q_x and ω depend on momentum $p_{//}$ and transverse betatron amplitudes $\hat{x}$ and $\hat{z}$.
In the following we will restrict ourselves to:

$$\omega = \omega(p_{//}) \quad \text{and} \quad Q_x = Q_x(p_{//}, \hat{x}) \tag{4}$$

Concerning the dependence on momentum, we introduce the following complementary definitions.

$$\xi = \frac{p_{//}}{Q_x}\frac{dQ_x}{dp_{//}} \text{ and } \omega_\xi = Q_{x0}\omega_0\frac{\xi}{\eta} \tag{5}$$

where ξ is called the machine chromaticity.

We develop $\dot{\varphi}$ with respect to the reference

$$p_{//0}\ ,\ Q_{x0}\ .$$

We assume an unperturbed longitudinal motion:

$$\tau = \tau_0 + \dot{\tau}t \text{ with constant } \dot{\tau}$$

and obtain

$$\dot{\varphi} = Q_x\omega = Q_{x0}\omega_0(1-\dot{\tau}) + \omega_\xi\dot{\tau} + \dot{\varphi}(\hat{x}) \tag{6}$$

$$\varphi = \int_0^t \dot{\varphi}dt + \varphi_0 = Q_{x0}\omega_0(t-\tau) + \omega_\xi\tau + \dot{\varphi}(\hat{x})t + \varphi_0 \tag{7}$$

Later on, we will perturb the motion by applying the transverse beam self field in the right-hand side of the equation of motion.

$$\ddot{x} + \dot{\varphi}^2 x = \frac{e}{m_0\gamma_0}\left[\vec{E} + \vec{v} \times \vec{B}\right]_\perp(t, \theta = \omega_0(t-\tau)) \tag{8}$$

In the $\{\varphi\ ,\ \hat{x}\}$ plane, the quantity of interest will be

$$\hat{\dot{x}} = \frac{d}{dt}\left[x^2+\left(\frac{\dot{x}}{\dot{\varphi}}\right)^2\right]^{\frac{1}{2}} = -\frac{\sin\varphi}{\dot{\varphi}}(\ddot{x} + \dot{\varphi}^2 x) \tag{9}$$

Therefore, the perturbed motion will be studied by means of:

$$\hat{\dot{x}} = -\frac{\sin\varphi}{\dot{\varphi}}\frac{e}{m_0\gamma_0}[\vec{E}+\vec{v}\times\vec{B}]_\perp(t,\theta=\omega_0(t-\tau)) \tag{10}$$

3. TRANSVERSE SIGNAL OF A SINGLE PARTICLE

The transverse PU electrodes deliver a signal proportional to the local beam centre-of-mass position and to the current.

$$S_\perp = S_{//}\, x_{CM} \tag{11}$$

Let us analyse the transverse signal of a single particle.

$$S_{//} = s_{//}(t,\theta) \tag{12}$$

The longitudinal signal consists of a series of periodic Dirac impulses with amplitude e and period

$$T = \frac{2\pi}{\omega} \tag{13}$$

The transverse amplitude is simply:

$$x = \hat{x}\cos\varphi(t) \tag{14}$$

therefore,

$$s_\perp(t,\theta) = e\hat{x}\sum_{k=-\infty}^{k=+\infty}\delta\left(t-\tau-\frac{\theta+2k\pi}{\omega}\right)\cos\varphi(t) \tag{15}$$

The signal display is sketched below.

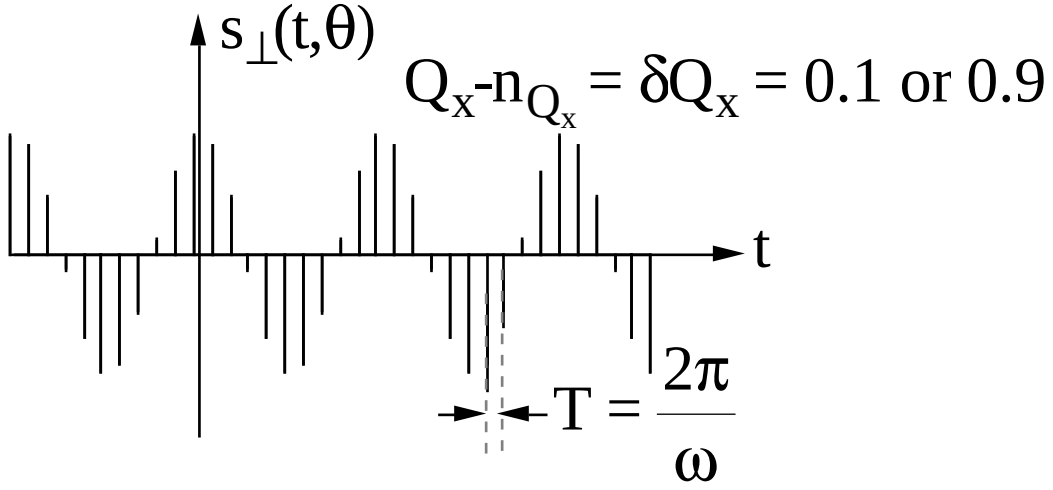

Fig. 3

The wave number is written as:

$$Q_X = n_{Q_X} + \delta Q_X \text{ with } n_{Q_X} \text{ the integer part}$$
$$\text{and } 0<\delta Q_X<1 \text{ the non integer part} \qquad (16)$$

Beam sampling at the position of the PU turn after turn makes it impossible to identify (modulo 1) the integer part $^{n}Q_X$ of the wave number. As a consequence, the same signal is obtained for

$$\delta Q_X \text{ and } 1 - \delta Q_X$$

After development of the series of Dirac's, the signal expression becomes:

$$s_\perp(t,\theta) = \frac{e\omega_0\hat{x}}{4\pi}\sum_{p=-\infty}^{p=+\infty} \exp -j(p\theta+\varphi_0)[\exp j\omega_p^+ t + \exp j\omega_p^- t] \qquad (17)$$

with two series of frequencies:

$$\omega_p^+ = (p+Q_X)\omega$$
$$\omega_p^- = (p-Q_X)\omega$$

Thus, in the spectrum, around every harmonic of the revolution frequency, there are two betatron (upper and lower) sidebands.

It is interesting to look for the incoherent frequency spread induced by a momentum spread and a betatron amplitude spread.

$$\delta\omega_p^+ = [(p+Q_{X0})\omega_0-\omega\xi]\dot{\tau} + \dot{\varphi}(\hat{x})$$
$$\delta\omega_p^- = [(p-Q_{X0})\omega_0+\omega\xi]\dot{\tau} - \dot{\varphi}(\hat{x}) \qquad (18)$$

The spread arising from momentum via the chromaticity varies with p. On the contrary, the spread due to amplitude spread is constant whatever the value p of the harmonic of the

revolution frequency.

As an example, for the lower sidebands, the incoherent spread due to momentum vanishes for

$$p = Q_{x0} - \frac{\omega\xi}{\omega_0} \tag{19}$$

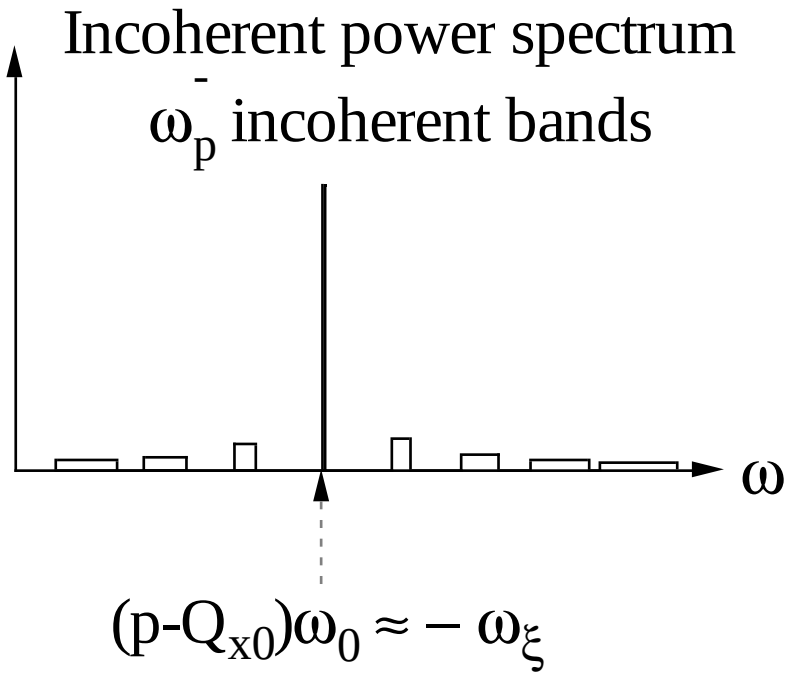

Fig. 4

As seen on the above figure, for this value of p the incoherent band is very narrow. The same picture would apply for the upper sidebands around $(p+Q_{x0})\omega_0 \approx \omega_\xi$.

A priori, these narrow betatron frequency bands represent a potential danger since there will be minimum Landau damping by momentum spread at this frequency. One will have to avoid chromaticity tunes which associate these narrow sidebands with large values of the transverse impedance.

In the following we will arbitrarily privilege the lower sidebands whenever it is necessary to solve the dispersion relation, or when we support our comments by figures. However, lower and upper sidebands are intimately linked and indissociable. We will further develop this fact in the following paragraphs.

4. DISTRIBUTION FUNCTION

To study transverse instabilities, we consider the following distribution:

$$\Psi(\varphi,\hat{x},\tau,\dot{\tau},t) = \Psi_0 + \Delta\Psi_p$$
$$g_0(\dot{\tau})f_0(\hat{x}) + g_p(\dot{\tau})f_p(\varphi,\hat{x})\exp j(p\omega_0\tau+\omega_{\perp pc}t) \tag{20}$$

The first term $\Psi_0 = g_0(\dot{\tau})f_0(\hat{x})$ is the stationary part normalized as follows:

$$\int_{\dot{\tau}} g_0(\dot{\tau})d\dot{\tau} = \frac{\omega_0}{2\pi} \text{ and } \int_{\hat{x}} f_0(\hat{x})\hat{x}d\hat{x} = \frac{1}{2\pi} \tag{21}$$

The second part $\Delta\psi p$ is the perturbation. Due to the τ dependence, it consists of a sinusoidal ($\exp j(p\omega_0\tau)$) transverse displacement of the beam with p wavelengths around the circumference.

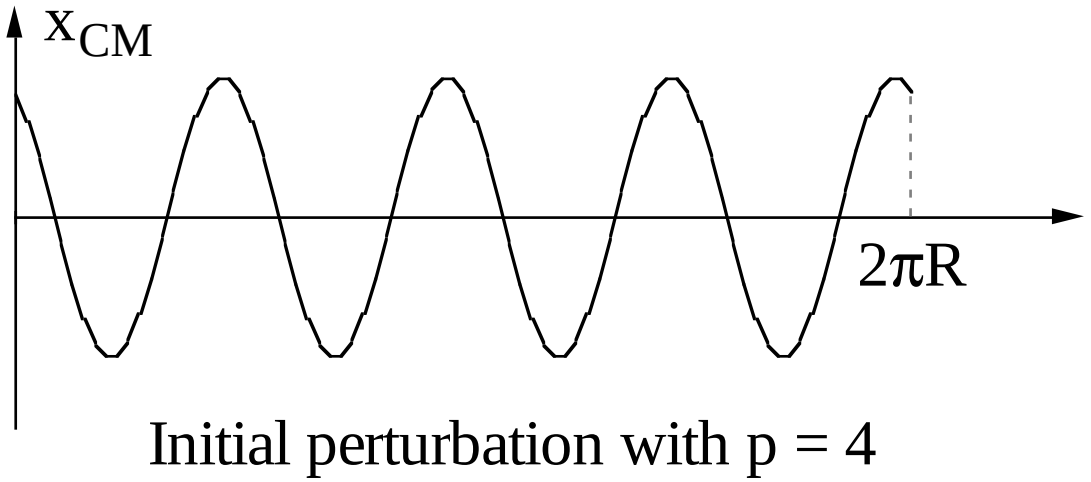

Fig. 5

It is also assumed that this perturbation will move at a coherent frequency $\omega_{\perp pc}$ apart from $p\omega_0$. The frequency offset $\omega_{\perp pc}$ is a complex number. For a lower sideband, we will write:

$$\omega_{\perp pc} = -Q_{x0}\omega_0 - \Delta Q_{xpc}\omega_0 \tag{22}$$

It is the sum of two quantities:

– the central incoherent $Q_{x0}\omega_0$ betatron frequency and,

– the coherent $\Delta Q_{xpc}\omega_0$ transverse betatron frequency shift.

The stability is evaluated from the expression

$$\text{Im}(\omega_{\perp pc}) = -\omega_0 \text{ Im}(\Delta Q_{xpc}) \tag{23}$$

5. TOTAL BEAM SIGNAL

In order to measure the total signal induced by the beam, one has to integrate the single particle signal over the distribution.

$$S_{\perp}(t,\theta) = \int_{v} \Psi(\varphi,\hat{x},\tau,\dot{\tau},t)s_{\perp}(t,\theta)dv \tag{24}$$

Let Σ represent the following integral:

$$\Sigma = \int_{\varphi,\hat{x},\dot{\tau}} g_p(\dot{\tau})f_p(\varphi,\hat{x})\hat{x}^2\cos\varphi \, d\varphi d\hat{x}d\dot{\tau} \tag{25}$$

Then, the transverse signal can be written:

$$S_{\perp}(t,\theta) = \frac{2\pi I\Sigma}{\omega_0} \exp j[(p\omega_0 + \omega_{\perp pc})t - p\theta] \tag{26}$$

in the time domain and,

$$S_{\perp}(\Omega,\theta) = \frac{2\pi I\Sigma}{\omega_0} \exp(-jp\theta)\, \delta(\Omega-(p\omega_0+\omega_{\perp pc})) \tag{27}$$

in the frequency domain. The chosen form of our perturbation leads to a single frequency line which will be used to probe the environment.

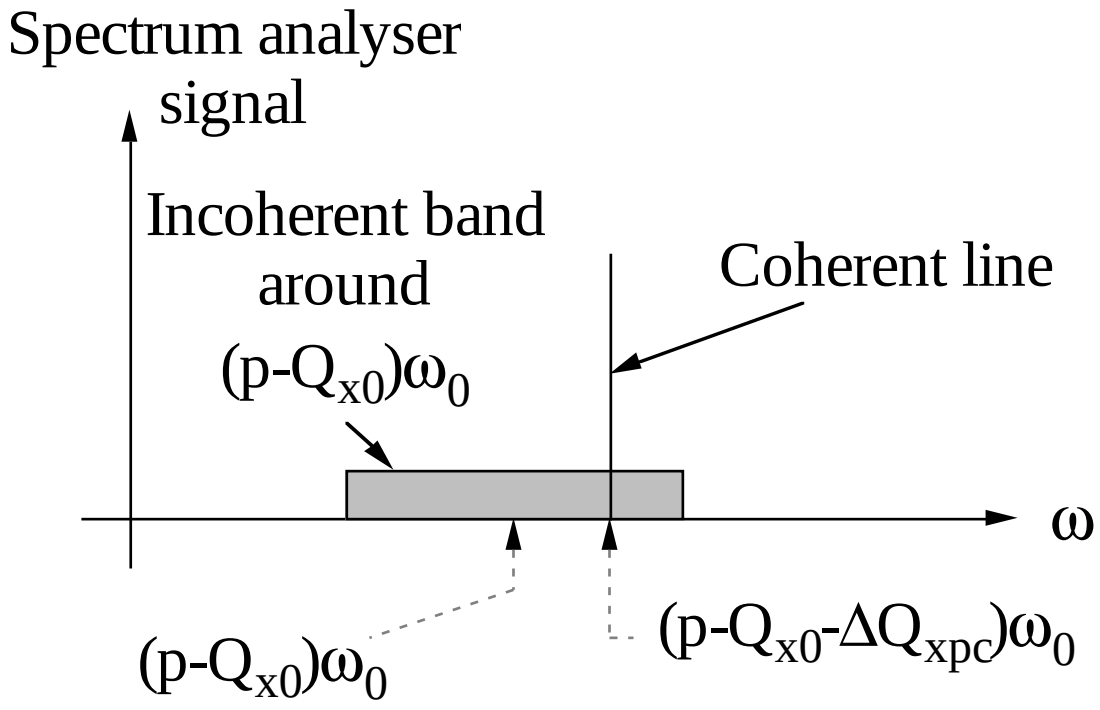

Fig. 6

6. DEFINITION OF TRANSVERSE COUPLING IMPEDANCE

Now we introduce the transverse coupling impedance. It relates transverse electromagnetic field and transverse signal at a given frequency as follows:

$$[\vec{E}+\vec{v} \times \vec{B}]_{\perp}(t,\theta) = \frac{-j\beta_0}{2\pi R} Z_{\perp} S_{\perp}(t,\theta) \tag{28}$$

with the units: the signal $S_{\perp}$ in Am and transverse impedance $Z_{\perp}$ in Ωm^{-1} .

The generalization to any signal is straightforward, it combines spectrum amplitude and impedance over the entire frequency range:

$$[\vec{E}+\vec{v} \times \vec{B}]_{\perp}(t,\theta) =$$
$$\frac{-j\beta_0}{2\pi R} \int_{\omega=-\infty}^{\omega=+\infty} Z_{\perp}(\omega) S_{\perp}(\omega,\theta) \exp(j\omega t)\, d\omega \tag{29}$$

In general, one cannot analytically express $Z_{\perp}(\omega)$. The solution of Maxwell's equations is never simple. To support the above definition, we just write down the results that one would tediously obtain for a continuous pipe of radius b through which a circular beam of constant radius a would travel.

For frequencies below the pipe cut-off frequency:

$$\omega \ll \omega_{\text{pipe cut-off}} = \frac{c}{b} \tag{30}$$

one could write:

$$[\vec{E}+\vec{v} \times \vec{B}]_{\perp}(t,\theta) = \frac{-j\beta_0}{2\pi R} \left(\frac{-jRZ_0}{\beta_0^2 \gamma_0^2} \left(\frac{1}{a^2} - \frac{1}{b^2} \right) \right) S_{\perp}(t,\theta) \tag{31}$$

provided the pipe wall is perfectly conducting $\sigma = \infty$.

The quantity between brackets is the transverse space-charge impedance:

$$Z_{\perp SC} = \frac{-jRZ_0}{\beta_0^2 \gamma_0^2} \left(\frac{1}{a^2} - \frac{1}{b^2} \right) \tag{32}$$

is a pure imaginary quantity and constant in the low frequency domain.

For a non-perfectly-conducting wall, $\sigma \neq \infty$, one has to add the resistive-wall contribution. One would find that the transverse and longitudinal resistive-wall impedances are linked by:

$$Z_{\perp RW} = \frac{2c}{b^2} \frac{Z_{//RW}}{\omega} \tag{33}$$

This handy formula is only valid for the resistive wall contribution of a circular pipe. It shows that the curves (impedance diagram)

$$Z_{\perp RW} \text{ and } \frac{Z_{//RW}}{\omega}$$

will be very similar.

For completeness, let us recall that

$$Z_{//RW} = (1+j)\,\frac{Z_0\beta_0}{2b}\,\delta_0\left(\frac{\omega}{\omega_0}\right)^{\frac{1}{2}} \tag{34}$$

in which $\delta_0 = \frac{2}{\mu\sigma\omega_0}$ is the skin depth at frequency ω_0.

7. TRANSVERSE COUPLING IMPEDANCE Z//(w) OF AN ACCELERATOR RING

In qualitative terms, observations made on several machines agree with the following description for the transverse coupling impedance of an accelerator ring. There are four major components. The space-charge impedance was already introduced in a previous section under crude assumptions. Below the pipe cut-off frequency its expression is:

$$Z_{\perp SC} = \frac{-jRZ_0}{\beta_0^2\gamma_0^2}\left(\frac{1}{a^2} - \frac{1}{b^2}\right) \tag{35}$$

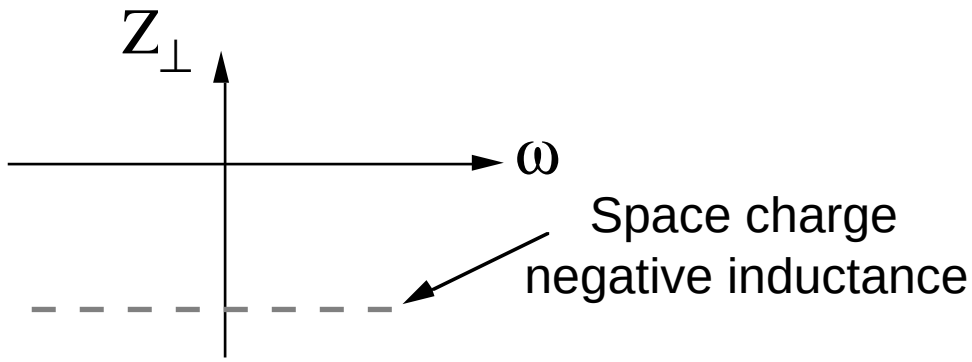

Fig. 7

It is a negative inductance large for slow particles in a pipe of small cross section.

The resistive-wall impedance was also previously mentioned. It will be shown later on that this component of the impedance is the main source of transverse instabilities. Provided the skin depth δ

$$\delta^2 = \frac{2}{\mu\sigma\omega} \tag{36}$$

at the considered frequency and ω is thinner than the wall thickness δ_w, then the resistive wall impedance can be expressed as:

$$Z_{\perp RW} = (1+j)\,\frac{RZ_0}{b^3}\,\delta_0\left(\frac{\omega_0}{\omega}\right)^{\frac{1}{2}} \tag{37}$$

At lower frequencies,

$$Z_{\perp RW} = \frac{2cR}{b^3\sigma\delta_w\omega} \tag{38}$$

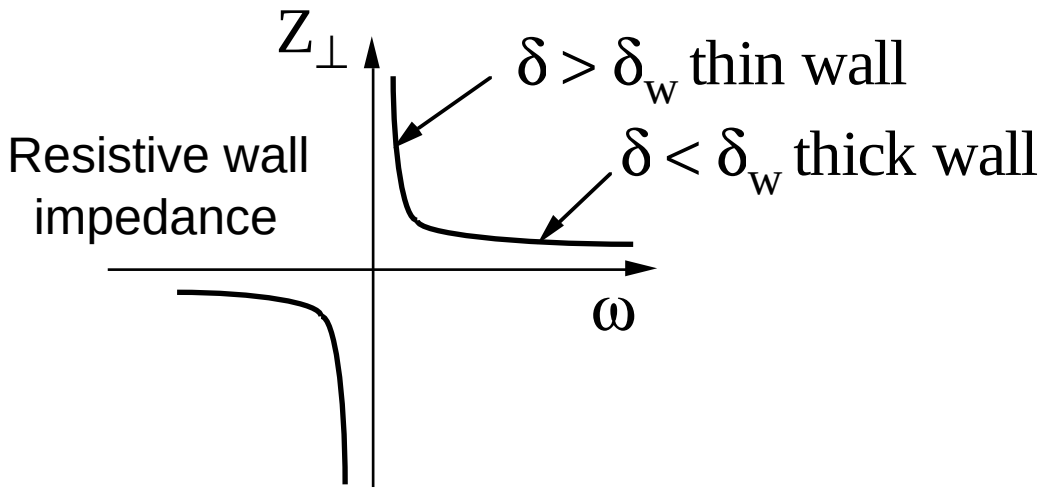

Fig. 8

Due to the b^3 dependence, machines with vacuum chambers of small cross section present a large impedance to the beam.

The third contribution to the machine impedance corresponds to high-Q resonators. As was the case for the longitudinal impedance, the main sources of such resonant objects are RF cavities.

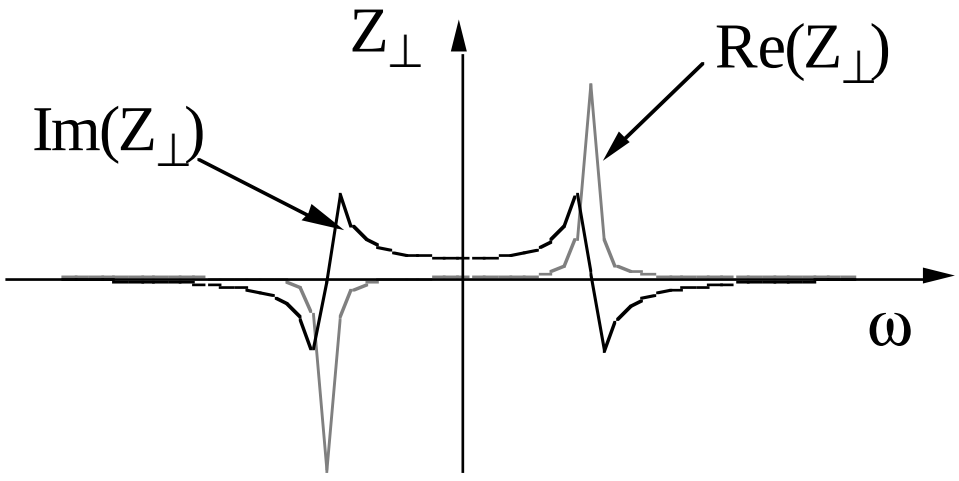

Fig. 9

With regard to the broad-band transverse impedance, up till now we have assumed a perfectly smooth circular pipe with neither cross section changes, bellows, nor flanges, etc. With a view to seeing the difference between an actual chamber and the circular pipe by means of a simple impedance model, it is common practice to introduce a transverse broad-band resonator.

A priori, there is no physical reason to believe that the parameters of this transverse broad.band resonator are linked to the parameters of the longitudinal broad-band resonator. However, measurements made on existing machines show that in the low frequency range the relation

$$Z_{\perp BB} = \frac{2c}{b^2}\frac{Z_{//BB}}{\omega} = \frac{2R}{\beta_0 b^2}\frac{Z_{//BB}}{p} \tag{39}$$

strictly valid for the resistive wake of a circular pipe, can lead to correct orders of magnitudes.

If one remembers that a typical range of longitudinal broad-band impedance value is:

$$0.2\ \Omega \le \left|\frac{Z_{//BB}}{p}\right| \le 50\ \Omega \tag{40}$$

then it can be concluded that the transverse broad-band impedance is in the MΩ/m range.

The scaling factor puts large machines with small vacuum chamber cross-section at a disadvantage. However, it is also easier to achieve the lowest values of $\left|\frac{Z_{//BB}}{p}\right|$ in large machines.

The use of a transverse broad-band impedance model to roughly simulate the effect of abrupt variations of the vacuum chamber, bellows, flanges, etc. leads to the introduction of:

- a positive inductance at low frequencies largely counterbalanced by the space-charge negative inductance for low energy machines,
- a resistive contribution around the pipe cut-off frequency,
- a capacitance at higher frequencies.

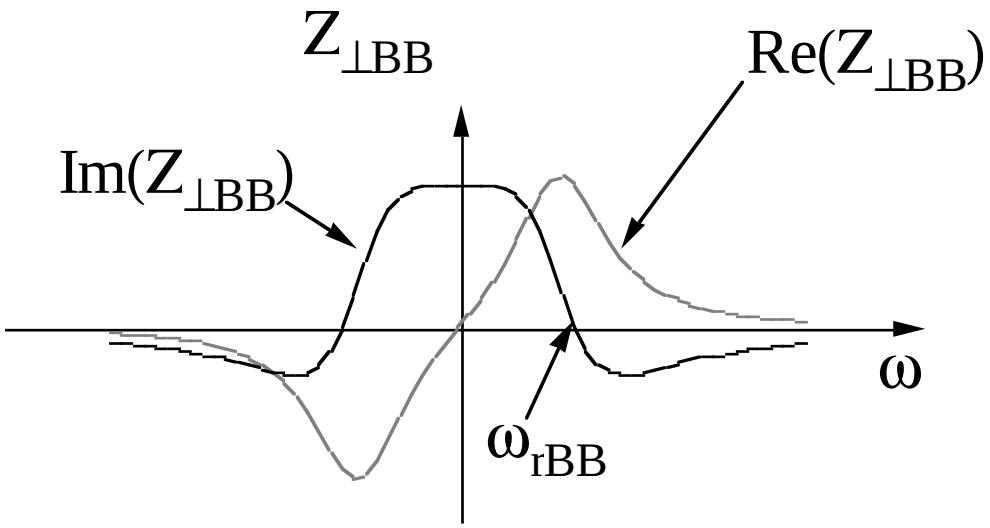

Fig. 10

At this stage it is necessary to point out an essential difference between transverse and longitudinal cases. The longitudinal motion is slow when compared to the revolution period. It takes many turns to perform a complete synchrotron oscillation and one can, in most cases, ignore the fact that some of the sources of impedance (RF cavities for instance) are localized.

In the transverse case, this approximation is not valid. A particle performs Q_{x0} oscillations per turn and the modulation of the amplitude function β_x cannot be ignored. The fact that particles are more (less) sensitive to impedance sources localised in high (low) β_x has to be taken into account. We can continue to assume a smooth machine with uniformly distributed focusing and impedance provided we introduce a kind of effective impedance to which localized objects contribute as follows:

$$Z_{\perp effective} = \frac{Q_{x0}}{R} \left(\beta_x Z_\perp\right)_{local} \tag{41}$$

As an example, the narrow transverse modes of RF cavities would contribute less if cavities were installed in low β_x straight sections.

8. DISPERSION RELATION FOR COHERENT MOTION

In this paragraph, we will gather all the results of previous paragraphs and then apply Vlasov's equation to find out consistent solutions for coherent motion. We will obtain a general dispersion relation. The solution of this equation will give the coherent frequency at which the perturbation oscillates.

$$\omega_{\perp pc} = -Q_{xpc}\omega_0 \tag{42}$$

The sign of the imaginary part will tell us whether coherent motion is stable or instable. Hereunder,the successive steps leading to the dispersion relation are summarized.

Distribution

$$\Psi(\varphi,\hat{x},\tau,\dot{\tau},t) = \Psi_0 + \Delta\Psi_p$$
$$g_0(\dot{\tau})f_0(\hat{x}) + g_p(\dot{\tau})f_p(\varphi,\hat{x})\exp\, j(p\omega_0\tau+\omega_{\perp pc}t) \tag{43}$$

Notation

$$\Sigma = \int_{\varphi,\hat{x},\dot{\tau}} g_p(\dot{\tau})f_p(\varphi,\hat{x})\hat{x}^2\cos\varphi\, d\varphi d\hat{x} d\dot{\tau} \tag{44}$$

Transverse signal

$$S_\perp(t,\theta) = \frac{2\pi I\Sigma}{\omega_0}\exp\, j[(p\omega_0 + \omega_{\perp pc})t - p\theta] \tag{45}$$

Electromagnetic field

$$[\vec{E}+\vec{v}\times\vec{B}]_\perp S_\perp(t,\theta) = \frac{-j\beta_0}{2\pi R} Z_\perp(p)S_\perp(t,\theta) \tag{46}$$

Differential equation for single-particle motion

$$\dot{\hat{x}} = -\frac{\sin\varphi}{\dot{\varphi}}\frac{e}{m_0\gamma_0}[\vec{E}+\vec{v}\times\vec{B}]_\perp(t,\theta=\omega_0(t-\tau)) \tag{47}$$

Vlasov's equation

$$\frac{d\Psi}{dt} = 0 = \frac{\partial\Psi}{\partial t} + \frac{\partial\Psi}{\partial\varphi}\dot{\varphi} + \frac{\partial\Psi}{\partial\hat{x}}\dot{\hat{x}} + \frac{\partial\Psi}{\partial\tau}\dot{\tau} + \frac{\partial\Psi}{\partial\dot{\tau}}\ddot{\tau}$$

$$\frac{\partial\Psi}{\partial t} = j\omega_{\perp pc}\, g_p(\dot{\tau})f_p(\varphi,\hat{x})\exp\, j(*)$$

$$\frac{\partial\Psi}{\partial\varphi}\dot{\varphi} = \dot{\varphi}\, g_p(\dot{\tau})\frac{\partial f_p(\varphi,\hat{x})}{\partial\varphi}\exp\, j(*)$$

$$\frac{\partial\Psi}{\partial\hat{x}}\dot{\hat{x}} = g_0(\dot{\tau})\frac{\partial f_0(\hat{x})}{\partial\hat{x}}\frac{\sin\varphi}{\dot{\varphi}}\frac{I\Sigma j Z_\perp(p)}{\frac{m_0\gamma_0 c}{e}}\exp\, j(*)$$
$$+ \text{neglected second order term} \tag{48}$$

$$\frac{\partial\Psi}{\partial t}\dot{\tau} = jp\omega_0\dot{\tau}\, g_p(\dot{\tau})f_p(\varphi,\hat{x})\exp\, j(*) \tag{49}$$

$$\ddot{\tau} = 0 \quad \text{no longitudinal electromagnetic field}$$

Intermediate equation

$$j(p\omega_0\dot{\tau}+\omega_{\perp pc})\, g_p f_p + \dot{\varphi} g_p \frac{\partial f_p}{\partial \varphi} = - g_0 \frac{\partial f_0}{\partial \hat{x}} \frac{\sin\varphi}{\dot{\varphi}} \frac{I\Sigma j Z_\perp(p)}{\frac{m_0\gamma_0 c}{e}} \tag{50}$$

In the perturbation $g_p f_p$ we separate the φ dependance on one hand and the $\hat{x}$ and $\dot{\tau}$ dependences on the other. In view of this, we introduce an intermediate function: $h(\hat{x},\dot{\tau})$ and write:

$$g_p(\dot{\tau}) f_p(\dot{\varphi},\hat{x}) = h(\hat{x},\dot{\tau}) \left(\cos\varphi - j \frac{\sin\varphi}{\dot{\varphi}} (p\omega_0\dot{\tau}+\omega_{\perp pc}) \right) \tag{51}$$

Vlasov's equation reduces to:

$$h(\hat{x},\dot{\tau}) = - \frac{I c \Sigma j Z_\perp(p)}{\frac{m_0\gamma_0 c^2}{e}} \frac{g_0 \frac{\partial f_0}{\partial \hat{x}}}{(p\omega_0\dot{\tau}+\omega_{\perp pc})^2 - \dot{\varphi}^2} \tag{52}$$

However, coming back to the original definition of Σ, one can also write:

$$\Sigma = \pi \int_{\hat{x},\dot{\tau}} h(\hat{x},\dot{\tau})\, \hat{x}^2 d\hat{x} d\dot{\tau} \tag{53}$$

In the previous expression of Vlasov's equation, after multiplication of both sides by $\pi\hat{x}^2$ and integration with respect to $\hat{x}$ and $\dot{\tau}$ one finally gets the dispersion relation:

$$1 = \frac{-\pi(\frac{q}{A}) I c}{(\frac{m_0 c^2}{e})\gamma_0} j Z_\perp(p) \int_{\dot{\tau},\hat{x}} \frac{g_0(\dot{\tau}) \frac{\partial f_0(\hat{x})}{\partial \hat{x}} \hat{x}^2}{(p\omega_0\dot{\tau}+\omega_{\perp pc})^2 - \dot{\varphi}^2} d\dot{\tau} d\hat{x} \tag{54}$$

In the next three paragraphs examples of solutions of the dispersion relation are given.

9. BEAM WITHOUT TUNE SPREAD

First, we assume a very cool beam in the longitudinal transverse plane: no momentum spread. In addition the wave number does not depend on the transverse betatron amplitude. In mathematical terms:

$$g_0(\dot{\tau}) = \frac{\omega_0}{2\pi}\,\delta(\dot{\tau}) \tag{55}$$

and

$$\dot{\varphi} = Q_{x0}\omega_0(1-\dot{\tau}) + \omega_\xi\dot{\tau} + \dot{\varphi}(\hat{x}) \text{ with } \dot{\varphi}(\hat{x}) = 0 \tag{56}$$

We use the following relation:

$$\int_{\hat{x}} \frac{\partial f_0(\hat{x})}{\partial \hat{x}}\hat{x}^2 d\hat{x} = -2\int_{\hat{x}} f_0(\hat{x})\,\hat{x}d\hat{x} = -\frac{1}{\pi} \tag{57}$$

and obtain:

$$(\omega_{\perp pc}^2 - Q_{x0}^2\omega_0^2) = \omega_0^2(Q_{xpc}^2 - Q_{x0}^2) = \frac{(\frac{q}{A})Ic}{2\pi(\frac{m_0c^2}{e})\gamma_0}\, jZ_\perp(p) \tag{58}$$

Q_{xpc}^2 is the coherent wave number.

The equation always has two roots (lower and upper sidebands):

$$\omega_{\perp pc}^{\pm} = Q_{\perp pc}^{\pm}\omega_0 \tag{59}$$

For small perturbations they are given by:

$$\mathrm{Re}(\omega_{\perp pc}^{\pm}) = \pm\left(Q_{x0}\omega_0 - \frac{(\frac{q}{A})Ic\ \mathrm{Im}\left(Z_\perp((p\pm Q_{x0})\omega_0\right)}{4\pi Q_{x0}(\frac{m_0c^2}{e})\gamma_0}\right) \tag{60}$$

$$\mathrm{Im}(\omega_{\perp pc}^{\pm}) = \pm\frac{(\frac{q}{A})Ic}{4\pi Q_{x0}(\frac{m_0c^2}{e})\gamma_0}\,\mathrm{Re}\left(Z_\perp((p\pm Q_{x0})\omega_0\right) \tag{61}$$

If the impedance has a resistive part, the coherent motion is always unstable.

The two series of coherent frequencies corresponding to lower and upper sidebands are solutions of the coherent motion:

$$\omega^+ = p\omega_0 + \omega_{\perp pc}^+ \quad \text{and} \quad \omega^- = p\omega_0 + \omega_{\perp pc}^- \tag{62}$$

Due to the properties of the impedance, for opposite values of the frequency ω:

$$\begin{aligned} \mathrm{Re}(Z_\perp(\omega)) &= -\,\mathrm{Re}(Z_\perp(-\omega)) \\ \mathrm{Im}(Z_\perp(\omega)) &= \mathrm{Im}(Z_\perp(-\omega)) \end{aligned} \tag{63}$$

both series lead to identical results. For instance one can look for conditions for instability:

$$\mathrm{Im}(\omega_{\perp pc}) < 0 \tag{64}$$

Unstable motion for the upper sidebands when

$$\omega^+ \approx (p + Q_{x0})\omega_0 \quad \text{is negative}$$

Unstable motion for the lower sidebands when

$$\omega^- \approx (p - Q_{x0})\omega_0 \quad \text{is positive}$$

This can be sketched in the impedance diagram:

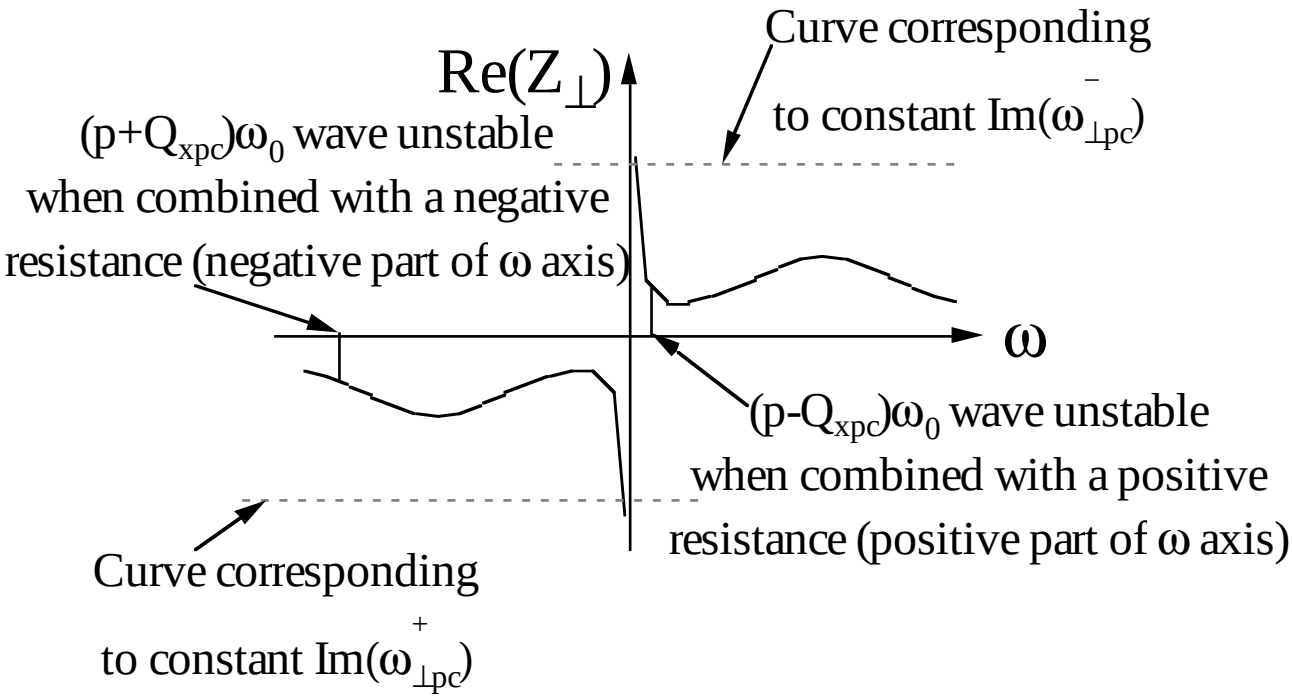

Fig. 11

In this figure, it is obvious that the transverse instability of a coasting beam is essentially a low frequency mechanism. This is because the beam is very sensitive to the low frequency region where the skin resistance tends to be very large, in particular much larger than the broad-band resistance.

In the stability diagram with

$$\mathrm{Re}(Z_\perp(w)) \text{ and } \mathrm{Im}(Z_\perp(-\omega))$$

coordinates, the curves corresponding to constant growth rate are vertical lines.

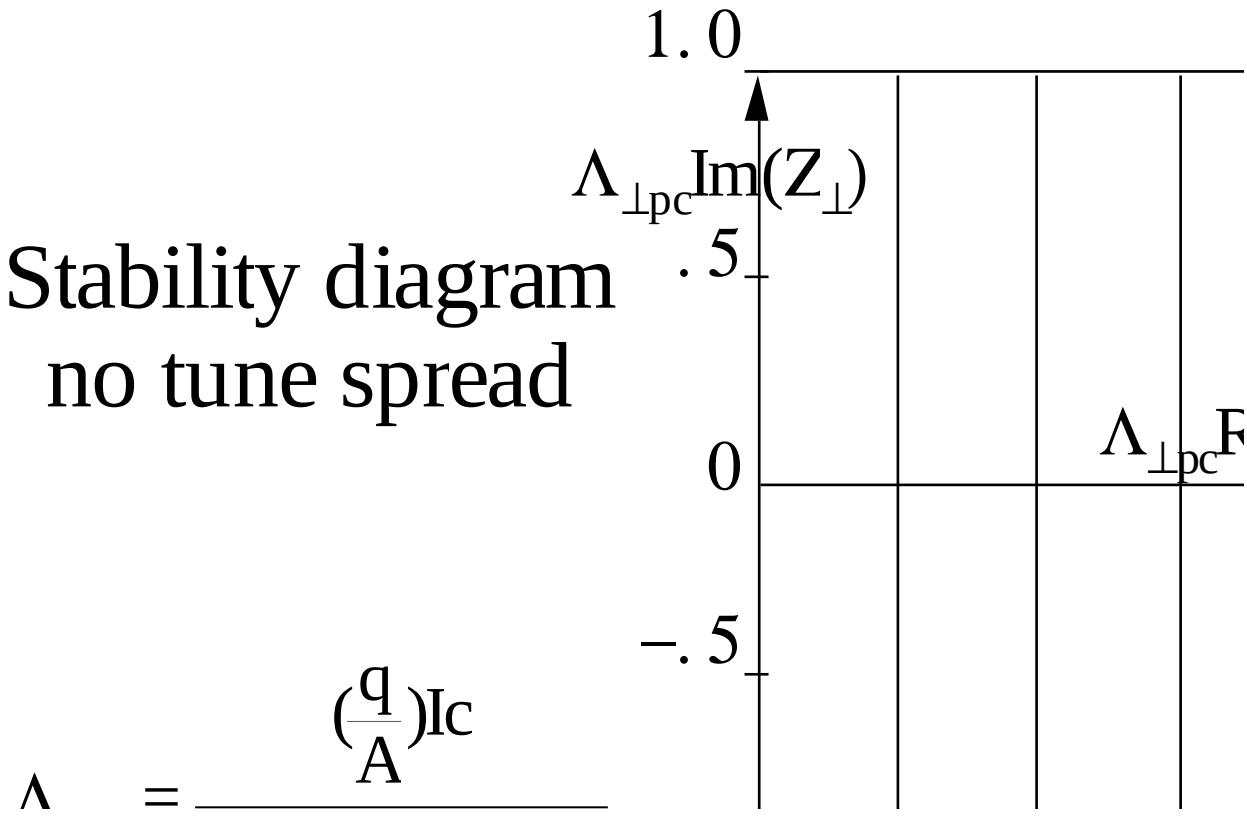

Fig. 12

The beam is always unstable except along the vertical axis. If the impedance were a purely imaginary number (inductance for instance), then the frequency shift would be real and coherent motion would be stable. In this respect, for the transverse plane we do not find the equivalent of the negative mass instability for the longitudinal plane.

When the beam is stable, a tune measurement device (RF knock out for instance) which necessarily detects the coherent motion only, indicates a certain value Q_{xpc} of the coherent wave number. A priori, our results indicate that Q_{xpc} is a linear function of beam intensity and one could imagine that the experimental curve Q_{xpc} versus current would allow the imaginary part of $Z_\perp(p)$ to be measured.

Unfortunately this is not the case. As a matter of fact, the space-charge contribution is not accessible and one will measure

$$\mathrm{Im}(Z_\perp - Z_{\perp SC})$$

This specificity of the space-charge component deserves some explanation. Let us assume a perfectly centered intense beam at low energy. The actual wave number of particles oscillating around the beam center, called incoherent wave number, is the result of two quadrupolar fields:

– the focusing of the external guide field

– the space-charge defocusing effect.

This incoherent wave number is the quantity noted Q_{x0} in this report. In other words:

$$Q_{x0} = Q_x \text{ external guide field} + \Delta Q_x \text{ space charge} \quad (65)$$

Obviously the tune is depressed by space-charge

$$\Delta Q_x \text{ space charge} < 0 \quad (66)$$

However, it must be pointed out that the space-charge field is null at the beam center. Now we rigidly displace the beam center and look for the coherent wave number. The beam center motion is influenced by:

– the focusing from the external guide field,
– the coherent deflecting magnetic field due to the broad-band inductance,
– the coherent deflecting field due to space-charge.

However, the space-charge field is still null at beam center. The coherent wave number logically compensates the incoherent tune depression due to space-charge.

As a conclusion, with a tune measurement device one cannot have access to $Z_{\perp SC}$ simply because the beam center of mass is not influenced by this field.

A practical remark can be made concerning the choice of the wave number. We have seen that the resistive wall impedance is likely to be the main source of instability. It behaves like

$$\omega^{-0.5}$$

in the thick wall assumption. It is therefore necessary to have the lowest coherent line at a frequency as high as possible

$$\omega \approx (p - Q_{x0})\omega_0$$

In view of this, with a tune 0.1 above an integer, the first coherent frequency line is at

$$\omega \approx 0.9\omega_0$$

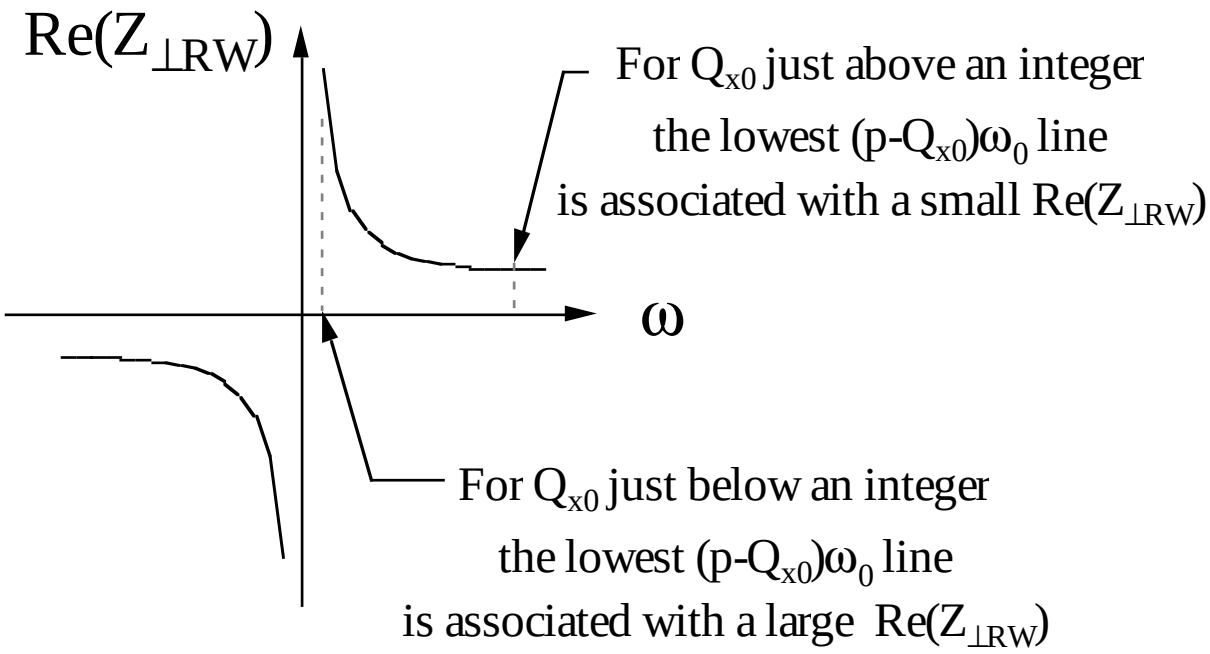

Fig. 13

On the contrary, with a tune of 0.9 (0.1 below the closest integer), this first coherent frequency line is at $\omega \approx 0.1\omega_0$. This factor 9 in frequency leads to a factor 3 in the value of corresponding resistive-wall impedance and consequently instability growth rate. Therefore, preference must be given to tunes just above an integer. As shown in this paragraph a beam with no spread in tune is always unstable. A spread in tune can provide the necessary Landau damping.

There are two principal possibilities for providing a tune spread:

- chromaticity via momentum spread, or
- transverse non linearities (tune variation with amplitude).

These two cases are studied independently in the two next paragraphs.

10. LANDAU DAMPING BY MOMENTUM SPREAD

We will assume a parabolic stationary distribution in momentum:

$$g_0(\dot{\tau}) = \frac{3\omega_0}{8\pi\dot{\tau}_L}\left(1 - \frac{\dot{\tau}^2}{\dot{\tau}_L^2}\right) \tag{67}$$

and solve the dispersion relation.

The denominator of the quantity in the integral can be written as the product of two terms

$$(\omega_{\perp pc} - Q_{x0}\omega_0 + ((p+Q_{x0})\omega_0 - w_\xi)\dot{\tau})$$
$$(\omega_{\perp pc} + Q_{x0}\omega_0 + ((p-Q_{x0})\omega_0 + w_\xi)\dot{\tau}) \tag{68}$$

They are associated with the upper (for the first one) and lower (for the second one) sidebands. We know from the previous paragraph that both waves lead to the same result. We will therefore concentrate on the slow wave (second term above) and look for the solution $\omega_{\perp pc} \approx -Q_{x0}\omega_0$. In this case, the first term above can be approximated by $-2Q_{x0}\omega_0$.

The then simplified dispersion relation can be written as follows:

$$1 = \frac{-(\frac{q}{A})Ic}{2Q_{x0}\omega_0(\frac{m_0c^2}{e})\gamma_0} jZ_\perp(p) \int_{\dot{\tau}} \frac{g_0(\dot{\tau})\, d\dot{\tau}}{\dot{\tau} + \frac{\omega_{\perp pc}+Q_{x0}\omega_0}{(p-Q_{x0})\omega_0+\omega_\xi}} \tag{69}$$

To simplify the writing we use the following definitions:

$$\Delta\omega_p = \left|(p-Q_{x0})\omega_0+\omega_\xi\right| \eta(\frac{\delta p}{p})_L \tag{70}$$

This quantity represents half the full width band (measured at the foot) of incoherent spread of frequency around the considered lower sideband line $(p-Q_{x0})\omega_0$.

$$\Lambda_{\perp pc} = \frac{3(\frac{q}{A})Ic}{16\pi Q_{x0}(\frac{m_0c^2}{e})\gamma_0\Delta\omega_p} \tag{71}$$

$$x_1 = -\frac{\omega_{\perp pc}+Q_{x0}\omega_0}{\Delta\omega_p} = \frac{(Q_{xpc}-Q_{x0})\omega_0}{\Delta\omega_p} = \frac{\Delta Q_{xpc}\omega_0}{\Delta\omega_p} \tag{72}$$

x_1 is the coherent betatron frequency shift normalized to the incoherent spread defined above.

We also use:

$$J_\perp = \int_{-1}^{+1} \frac{1-x^2}{x-x_1}\,dx \tag{73}$$

With these notations the dispersion relation can be finally written:

$$\frac{1}{J_\perp} = \Lambda_{\perp pc}\, jZ_\perp(p) \tag{74}$$

The stability diagram with:

$$\Lambda_{\perp pc}\ \mathrm{Re}(Z_\perp(p)) \text{ and } \Lambda_{\perp pc}\ \mathrm{Im}(Z_\perp(p))$$

along the axes is shown in Fig. 14.

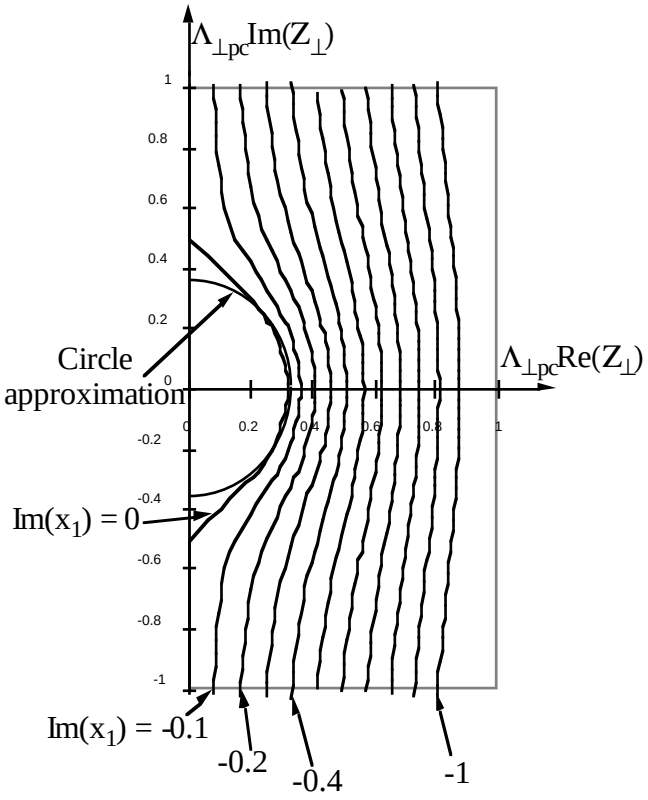

Fig. 14

The imaginary part of the coherent frequency is positive and the movement is damped for small values of the transverse impedance. When compared to the previous example of a monochromatic beam, provided the impedance is reasonably small, the incoherent frequency spread arising from momentum can stabilize the coherent motion. On the contrary, for large $|Z_\perp(p)|$ Landau damping is not strong enough and coherent motion is instable. The curve $\mathrm{Im}(x_1) = 0$ defines the stability limit. Its contour can be approximated by a circle:

$$|\Lambda_{\perp pc} Z_\perp(p)| < \frac{3\sqrt{2}}{4\pi} F \tag{75}$$

with $F \approx 1$ for the assumed parabolic distribution.

Although the detailed form of the stability limit curve depends on the exact momentum distribution function, very similar results would be obtained for other realistic distribution functions with the same $(\frac{\delta p}{p})_{FWHH}$. The criterion can be rewritten in terms of the incoherent spread. We will use the FWHH as a reference:

$$\Delta\omega_{p\ FWHH} = \sqrt{2}\Delta\omega_p \tag{76}$$

Then stability requires:

$$\Delta\omega_{p\ FWHH} > \frac{(\frac{q}{A})Ic|Z_\perp(p)|}{4Q_{x0}(\frac{m_0c^2}{e})\gamma_0} \tag{77}$$

It is interesting to note that the quantity on the right hand side of the above relation can be very simply linked with the coherent betatron frequency shift one would obtain with a monochromatic beam (cf previous paragraph).

$$\Delta\omega_{p\ FWHH} > \pi\omega_0 |Q_{xpc}-Q_{x0}|_{\substack{\text{monochromatic}\\ \text{beam}}} \tag{78}$$

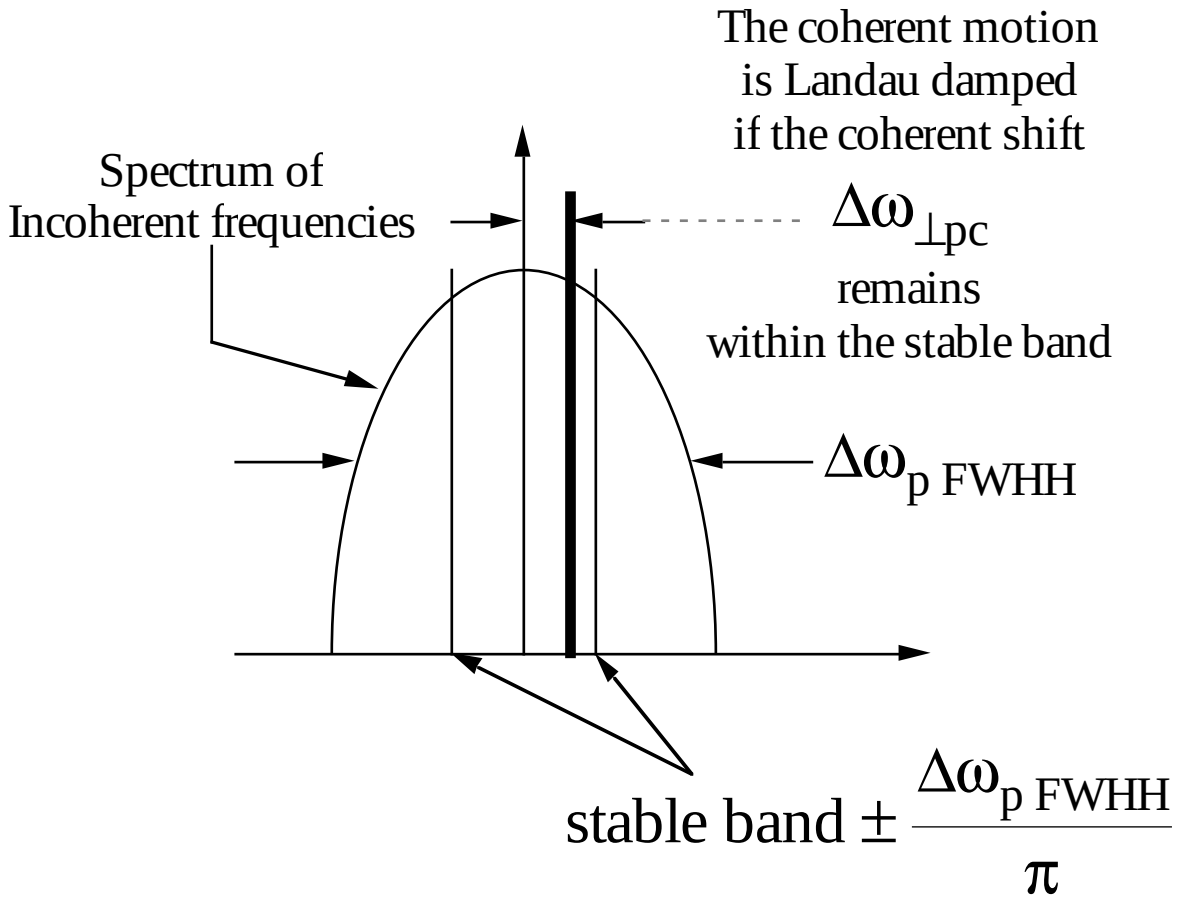

Fig. 15

For standard uncorrected optics, $\xi \approx -1$ and $\omega_\xi = \frac{Q_{x0}\omega_0}{\eta}$ are negative above

transition. This corresponds to the worst situation because

$$\Delta\omega_{p\ FWHH} = \left((p-Q_{x0})\omega_0+\omega\xi\right)\left|\eta\left(\frac{\delta p}{p}\right)_{FWHH}\right|$$

$$p \approx Q_{x0}\left(1 - \frac{\xi}{\eta}\right)$$
vanishes around .

To improve the situation, one has to change the sign of the chromaticity by introducing sextupoles in the dispersive sections of the lattice. Correction of chromaticity in both planes is not always simple in particular in large machines. The non-linearities generated by the sextupoles can severely limit the single particle dynamic acceptance of the machine. The optimization of the sextupolar correction scheme is often very challenging. It can largely influence the choice of the basic linear optics.

It must be pointed out that transverse stability of coherent motion is not necessarily the only reason to correct chromaticity. When the uncorrected ξ is large, the incoherent tune spread due to momentum is also large. In a tune diagram, space between dangerous betatron resonances is always limited.

For machines working below transition, the natural chromaticity is in general positive and has therefore the right sign to always provide some Landau damping. In the impedance diagram, one can draw the line which represents the incoherent frequency band $\Delta\omega_{p\ FWHH}$ as a function of ω. .

It can be seen that the low frequency region is the most dangerous and for two reasons. The resistive wall impedance is large and the frequency band is narrow.

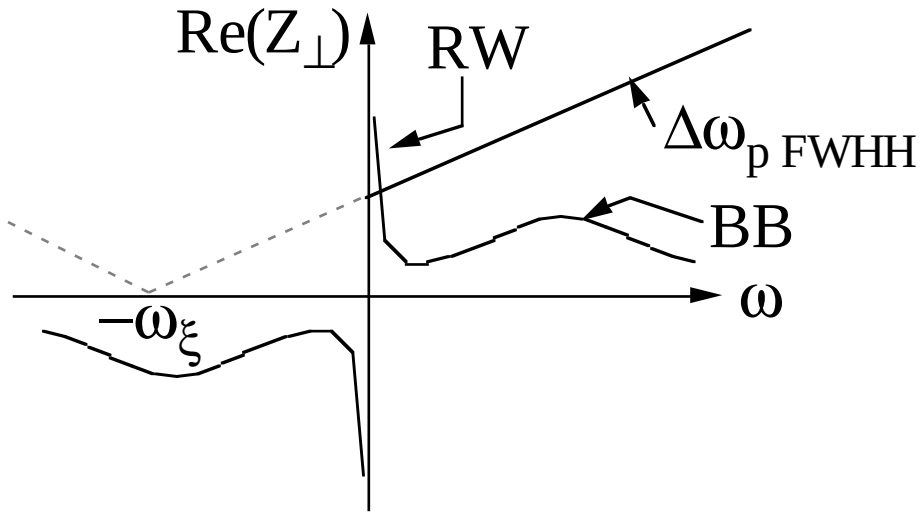

Fig. 16

This is the reason why transverse instability is currently a low-frequency mechanism. If Landau damping is insufficient, coherent motion can also be stabilized by a feedback system. Fortunately, the conception of such a system is easier at low frequency.

1. LANDAU DAMPING BY AMPLITUDE DEPENDENT TUNE

Now we separately consider the influence of a tune spread arising from a betatron amplitude spread in the beam. In order to write down the corresponding dispersion relation, we assume a monochromatic beam:

$$g_0(\dot{\tau}) = \frac{\omega_0}{2\pi}\,\delta(\dot{\tau}) \tag{80}$$

and for instance a parabolic distribution of betatron amplitudes:

$$f_0(\hat{x}) = \frac{2}{\pi \hat{x}_L^2}\left(1 - \left(\frac{\hat{x}}{\hat{x}_L}\right)^2\right) \text{ for } 0 < \hat{x} < \hat{x}_L$$

and

$$f_0(\hat{x}) = 0 \text{ for } \hat{x} > \hat{x}_L \tag{81}$$

Under these assumptions, the dispersion relation takes the following form:

$$1 = \frac{-\left(\frac{q}{A}\right)Ic}{2\pi Q_{x0}\omega_0\left(\frac{m_0c^2}{e}\right)\gamma_0\Delta Q_L}\, jZ_\perp(p)\int_0^1 \frac{x\,dx}{x - \frac{\Delta Q_{xpc}}{\Delta Q_L}} \tag{82}$$

The following definition:

$$\Delta Q_L = \frac{\partial Q_x}{\partial \hat{x}^2}\,\hat{x}_L^2 \tag{83}$$

is used to measure the total incoherent tune spread due to amplitude in the beam. We then note:

$$x_1 = \frac{\Delta Q_{xpc}}{\Delta Q_L} \tag{84}$$

This complex number measures the coherent tune shift in total incoherent tune spread units. The integral can then be written:

$$J_\perp = \int_0^1 \frac{x\,dx}{x - x_1} \tag{85}$$

We also note

$$\Lambda_{\perp pc} = \frac{-\left(\frac{q}{A}\right)Ic}{2\pi Q_{x0}\omega_0\left(\frac{m_0c^2}{e}\right)\gamma_0\Delta Q_L} \tag{86}$$

and are left with

$$\frac{1}{J_\perp} = \Lambda_{\perp pc} j Z_\perp(p) \tag{87}$$

As was already done in the previous examples, the solutions can be worked out by drawing the curves corresponding to a given value of $\mathrm{Im}(x_1)$ in the stability diagram.

$$\begin{aligned} \Lambda_{\perp pc}\mathrm{Re}(Z_\perp(p)) &= \mathrm{Im}\left(\frac{1}{J_\perp}\right) \\ \Lambda_{\perp pc}\mathrm{Im}(Z_\perp(p)) &= -\mathrm{Re}\left(\frac{1}{J_\perp}\right) \end{aligned} \tag{88}$$

The results are shown in Fig. 17.

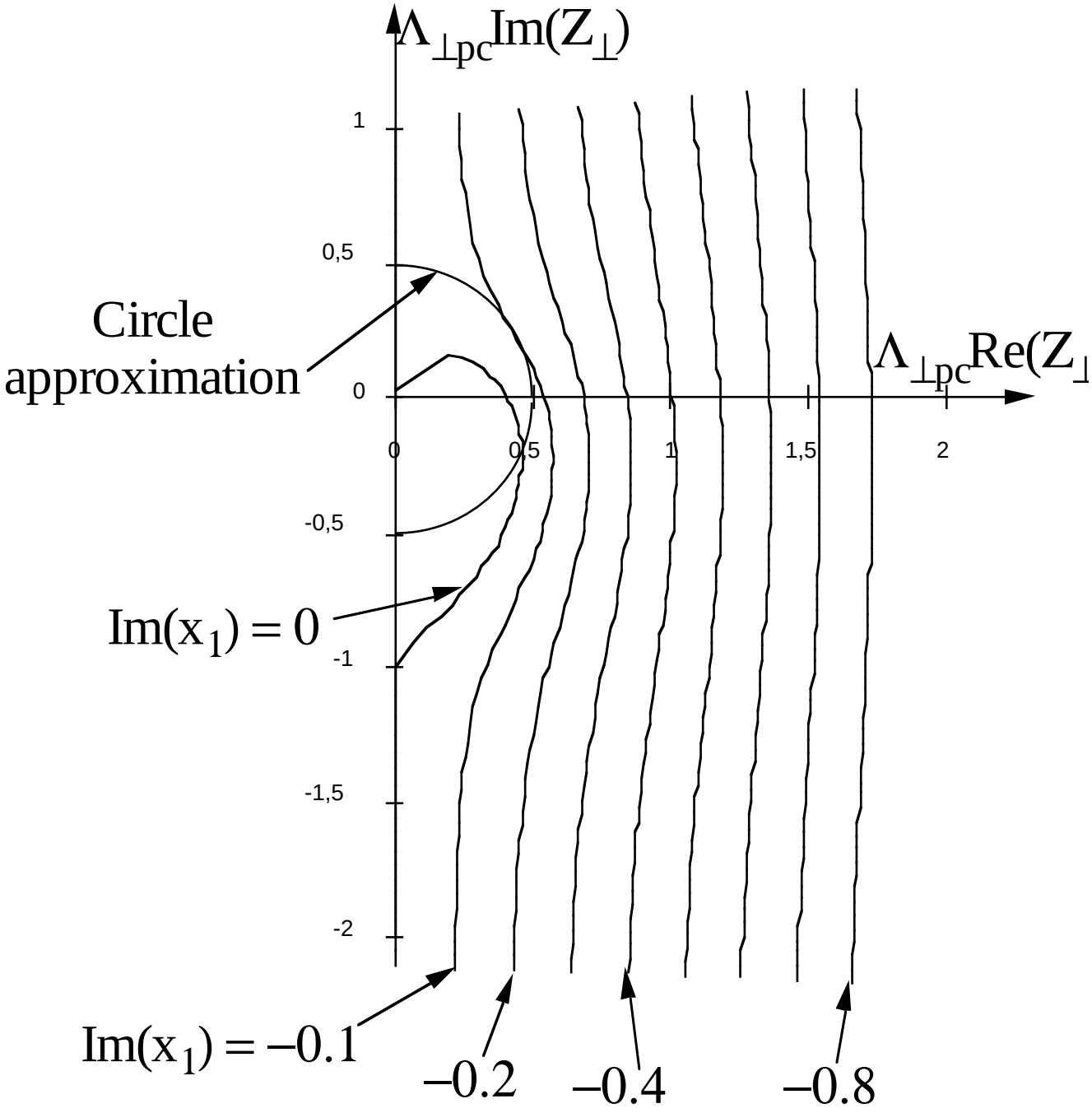

Fig . 17

As already mentioned, the details of the stability contour depend on the tails of the distribution. The transverse distribution enters the integral via its derivative $\frac{\partial f_0}{\partial \hat{x}}$ which for the specific suggested example presents a discontinuity at the edges. This explains the heart shape of the stability contour which would be much less pronounced, and even not exist, for a smoother distribution. In view of this, we suggest using

$$\left|\Lambda_{\perp pc} Z_\perp(p)\right| < 0.5 \tag{89}$$

as an approximation of the stability criterion. The interpretation is very similar to that

given in the previous paragraph for a momentum spread. When the incoherent tune spread due to amplitude spread is large enough,

$$\Delta Q_L \omega_0 = \Delta \omega_{p\ L} > \frac{(\frac{q}{A}) I c |Z_\perp(p)|}{\pi Q_{x0} (\frac{m_0 c^2}{e}) \gamma_0} \tag{90}$$

coherent motion is Landau damped.

If one compares the above result with that previously obtained for a momentum spread,

$$\Delta \omega_{p\ FWHH} > \frac{(\frac{q}{A}) I c |Z_\perp(p)|}{4 Q_{x0} (\frac{m_0 c^2}{e}) \gamma_0} \tag{91}$$

$$\text{with } \Delta \omega_{p\ FWHH} = \left((p - Q_{x0}) \omega_0 + \omega_\xi \right) \left| \eta \left(\frac{\delta p}{p} \right)_{FWHH} \right| \tag{92}$$

apart from the distinction between the definitions used for FWHH and total (L), the main difference is that the width of the incoherent band due to amplitude spread is now independent of p. Another way to summarize the results is to express the necessary incoherent spread in terms of the coherent betatron frequency shift one would obtain with a monochromatic beam.

$$\Delta \omega_{p\ L} > 4\ \omega_0 \left| Q_{xpc} - Q_{x0} \right|_{\substack{\text{monochromatic} \\ \text{beam}}} \tag{93}$$

BIBLIOGARPHY

C.E. Nielsen et al., Proc. of Int. Conf. on High Energy Accel. and Instr., CERN (1959) 239

V.K. Neil, R.J. Briggs, Plasma Physics, 9 (1967) 631

V.K. Neil, A.M. Sessler, Rev. Sci. Instr. 36 (1965) 429

B.W. Montague, Single Particle Dynamics, 3rd lecture, Int. School of Particle Accel., Erice (1976)

B.W. Montague, Single Particle Dynamics, 5th and 6th lectures, Int. School of Particle Accel., Erice (1976)

H.G. Hereward, Landau Damping, Int. School of Particle Accel., Erice (1976)

K. Hübner, V.G. Vaccaro, CERN report ISR-TH/70-44 (1970)

B. Zotter, CERN report ISR-GS/76-11 (1976)

A.G. Ruggiero, V.G. Vaccaro, CERN report ISR-TH/68-33 (1968)

E. Keil, W. Schnell, CERN report ISR-TH-RF/69-48 (1969)

F. Sacherer, Proc. 1973 Part. Accel. Conf., San Francisco, IEEE Trans. Nucl. Sci. Vol. NS-20, n°3, 825

F. Sacherer, CERN report SI/BR/72-5 (1972)

A. Hofmann, Single Beam collective phenomena-longitudinal, Int. School of Part. Accel., Erice (1976)

I. Hofmann, Non linear aspects of Landau damping in computer simulation of the microwave instability, Computing in Accelerator Design and Operation, Berlin, Sept. 20-23 1983

J.L. Laclare, Bunched-beam instabilities, 11th Int. conference on High Energy Accelerators, Geneva (July 1980) 526

J.L. Laclare, Instabilities in storage rings, Proc. of the Symposium on Accelerator Aspects of H I Fusion, Darmstadt FRG (1982), GSI Report 82-8.